American Journal of Pathology, Vol. 159, No. 2, August 2001

The Perifollicular and Marginal Zones of the Human Splenic White Pulp

Do Fibroblasts Guide Lymphocyte Immigration?

Birte Steiniger,* Peter Barth,† and Achim Hellinger‡

From the Institute of Anatomy and Cell Biology, University of Marburg, Marburg; and the Departments of Pathology† and Surgery,‡ University Hospital of Marburg, Marburg, Germany*

We investigate the white pulp compartments of 73 human spleens and demonstrate that there are several microanatomical peculiarities in man that do not occur in rats or mice. Humans lack a marginal sinus separating the marginal zone (MZ) from the follicles or the follicular mantle zone. The MZ is divided into an inner and an outer compartment by a special type of fibroblasts. An additional compartment, termed the perifollicular zone, is present between the follicular MZ and the red pulp. The perifollicular zone contains sheathed capillaries and blood-filled spaces without endothelial lining. In the perifollicular zone, in the outer MZ, and in the T cell zone fibroblasts of an unusual phenotype occur. These cells stain for the adhesion molecules MAdCAM-1, VCAM-1 (CD106), and VAP-1; the Thy-1 (CD90) molecule; smooth muscle α-actin and smooth muscle myosin; cytokeratin 18; and thrombomodulin (CD141). They are, however, negative for the peripheral node addressin, the cutaneous lymphocyte antigen, CD34, PECAM-1 (CD31), and P- and E-selectin (CD62P and CD62E). In the MZ the fibroblasts are often tightly associated with CD4-positive T lymphocytes, whereas CD8-positive cells are almost absent. Our findings lead to the hypothesis, that recirculating CD4-positive T lymphocytes enter the human splenic white pulp from the open circulation of the perifollicular zone without crossing an endothelium. Specialized fibroblasts may attract these T cells and guide them into the periarteriolar T cell area. ***(Am J Pathol 2001, 159:501–512)***

The normal microscopic anatomy of human spleens is still highly controversial, both in the literature and in anatomy or pathology textbooks. Although several immunohistological investigations exist,[1–6] there is, for example, no consensus about the compartments constituting the white pulp or about the ramifications of the microvasculature. This is primarily because of the fact that the well-known features of splenic microarchitecture in laboratory rodents[7–10] are assumed to be also present in humans. Precise knowledge of splenic microanatomy is needed, because the spleen is the most important organ for lymphocyte recirculation in humans. Moreover, the spleen is equipped with a unique type of microcirculation permitting lymphocytes to exit from the blood under conditions of low shear stress and in the absence of high endothelial venules (HEVs).

In mammals the white pulp of the spleen is composed of three compartments, the periarteriolar lymphatic sheath (PALS), the follicles, and the marginal zone (MZ). The PALS is a T cell compartment directly surrounding the so-called central arterioles. The follicles and the MZ represent areas of B cell predominance.

The prevalent picture of splenic white pulp microanatomy has been derived from rats. In this species the MZ ensheathes the PALS and the follicles. The MZ exists of a thick cell layer primarily composed of a special type of memory B cells expressing IgM but no IgD or only minor amounts. Primary follicles represent accumulations of small strongly IgD-positive recirculating B lymphocytes, attached to the PALS at regular intervals. The intense expression of surface IgD serves as a hallmark of recirculating B cells.[11] Primary follicles have a uniform internal structure, whereas secondary follicles consist of a pale inner germinal center with centroblasts and centrocytes. The surrounding corona or mantle zone represents the remainder of the primary follicle and harbors the small recirculating B lymphocytes.

In rats a rather leaky branched microvessel, the marginal sinus, is supposed to mediate lymphocyte entry from the blood into the white pulp. The marginal sinus forms a visible border between the PALS and the follicles on one side and the MZ on the other. Its visibility is because of the accompanying pale-staining marginal metallophilic macrophages. In addition, the MZ contains a second population of macrophages, the MZ macrophages that are scattered all over the compartment. Both types of macrophages express sialoadhesin, an adhesion molecule of the siglec family.[12]

Accepted for publication March 29, 2001.

Address reprint requests to Prof. Birte Steiniger, Institute of Anatomy and Cell Biology, Robert-Koch-Str. 6, D-35033 Marburg, Germany. E-mail: steinigb@mailer.uni-marburg.de.

Table 1. Human Spleens Removed *ex Vivo*

Diagnosis	Number of organs
Polytrauma with blunt abdominal trauma	30
Iatrogenic splenic lesion	1
Gastrointestinal malignancies	14
Thrombocytopenia	2
Pancreatitis	1
Diverticulosis	1
Other trauma, attempted suicide	2
Vascular tumour of spleen	1
Multi-organ donor	11

Our previous results show that the microanatomy of the human splenic white pulp differs from that of rats in four major aspects.[13] First, in adult humans, primary B cell follicles occupy most of the white pulp area. The PALS is only sparsely distributed and tends to occur around larger arteries. Central arterioles may run directly through follicles without being covered by T cells at all. Second, the human MZ is primarily present around the follicles and only a few B lymphocytes occur along the PALS. Third, the MZ is not separated from the primary follicles or from the mantle zone of secondary follicles, because a marginal sinus is absent in humans. Fourth, there is an additional region outside the MZ, the perifollicular zone, where blood occurs in a compartment belonging to the open splenic circulation.

In this study, we analyze, whether the microanatomical differences between rats and humans also extend to cells and adhesion molecules that may serve lymphocyte immigration from the blood into the splenic white pulp. We explore how recirculating lymphocytes may be guided into the white pulp if a marginal sinus is indeed absent in humans.

Materials and Methods

Human Spleens

Specimens from 73 individuals (44 males and 29 females) were investigated. Thirty-one specimens came from individuals younger than 35 years of age. The diagnoses leading to removal of the spleen are summarized in Table 1. With the exception of four cases, splenic weights of abdominal trauma patients were <200 g. Twenty-six trauma patients were younger than 40 years of age. The trauma patients had no additional histopathological diagnoses with the exception of two patients with accompanying gastrointestinal inflammation. Spleen and pancreas of multiorgan donors were perfused *in situ* with University of Wisconsin preservation solution (Viaspan, Dupont, Bad Homburg, Germany). In 10 additional cases specimens were obtained postmortem. Of these, five patients had malignancies, three had cardiovascular diseases, one died from CO-intoxication and one from cerebral hemorrhage. The organs had been either fixed in 4% formalin in tap water ($n = 61$) for an unknown duration or they were kept in Baker's formol-calcium for 24 hours ($n = 12$) and were immediately embedded in paraffin. Nine specimens were additionally frozen and stored in liquid nitrogen within 4 hours after removal of the organ.

Antibodies

The primary antibodies used are summarized in Table 2. All organs were embedded in paraffin and were stained with the panel of reagents suitable for this material (see below). The monoclonal antibody (mAb) against smooth muscle myosin was only applied to a smaller number of specimens. In addition, the nine frozen specimens were also tested with all reagents except for antibodies against CD79a and CD4, which did not work on cryosections. The antibody against smooth muscle myosin was not tried on cryosections.

Biotinylated goat-anti-rabbit IgG (no. BA-1000) and the ABC elite kit (no. PK-6102) were bought from Vector Laboratories, Burlingame, CA, via Camon, Wiesbaden, Germany.

Single-Staining Procedure for Immunohistology

All antibodies were tested for reactivity on paraffin and cryostat sections. If possible, both types of sections were investigated. This is essential, because formalin fixation often leads to reduced antibody staining in paraffin sections. On the other hand, the resolution of cryosections is sometimes too low to permit unequivocal identification of splenic compartments.

CD14, CD15, KiM2, CD62E, CD62P, CD90, CD106, and prolyl-hydroxylase were only detectable in cryostat sections, whereas CD79a and CD4 were only studied in paraffin sections. Both MAdCAM-1 antibodies gave a strong reaction in cryosections. 10A6 was also weakly positive on paraffin-embedded material, whereas 10G3 did not react. All antibodies were detected using the Vectastain ABC elite kit.

Paraffin sections were deparaffinized, washed in bidistilled water, and incubated in 0.05% proteinase type XIV (Sigma no. P-5147) in Tris/NaCl, pH 7.6, for 15 minutes at room temperature. After washing in phosphate-buffered saline (PBS) the sections were covered with H_2O_2 solution at a final concentration of 0.15% in PBS for 30 minutes at room temperature to block peroxidatic activity. Cryostat sections were fixed in cold isopropanol for 10 minutes and pretreated with 0.4 U/ml glucose oxidase in PBS with 10 mmol/L glucose and 1 mmol/L NaN_3 at 37°C for 45 minutes. The primary antibodies were used at dilutions between 1:100 and 1:800 in PBS containing 1% bovine serum albumin, 0.1% NaN_3, and a final concentration of 3 μg/ml avidin (Sigma no. A-9275) and incubated with the washed sections overnight at 4°C. Biotinylated goat anti-rabbit or anti-mouse IgG was diluted 1:200 in PBS with a final concentration of 20 μg/ml biotin (Sigma no. B-4501). After washing the sections were incubated with this solution for 30 minutes at room temperature. The avidin-biotinylated peroxidase complex was prepared according to the manufacturer's instructions 30 minutes before use. The sections were washed and incubated with the avidin-biotinylated peroxidase

Table 2. Antibodies

mAb	Specificity	Producer/distributor	Reference
28	Human CD15, 3-fucosyl-*N*-acetyl-lactosamine (Le^x) residue, present in several membrane molecules on monocytes and granulocytes	Cymbus Biotechnology, Chandlers Ford, UK, no. CBL 144, via Dianova, Hamburg, Germany	
1.2B6	Human CD62E (E-selectin)	DAKO, Hamburg, Germany, no. M 7105	
1.4C3	Human CD106 (VCAM-1)	Serotec, Oxford, UK, no. MCA 981, via Biozol, Eching, Germany	
1E3	Human CD62P (P-selectin)	DAKO, Hamburg, Germany, no. M 7199	
1F6	Human CD4	Novocastra, Edinburgh, UK, no. NCL CD4/CD8, via Medac, Hamburg, Germany	
4B11	Human CD8	Novocastra, Edinburgh, UK, no. NCL CD4/CD8, via Medac, Hamburg, Germany	
5B5	Human prolyl-4-hydroxylase (EC 1.14.11.2)	DAKO, Hamburg, Germany, no. M 0877	
10A6	Human MAdCAM-1	Donated by Dr. M. Briskin, LeukoSite Inc., Cambridge, USA	Briskin et al[14]
10G3	Human MAdCAM-1	Donated by Dr. M. Briskin, LeukoSite Inc., Cambridge, USA	Briskin et al[14]
AS02	Human CD90 (Thy-1)	Dianova, Hamburg, Germany, no. dia 100	Saalbach et al[15]
asm-1	Smooth muscle α-actin	Progen GmbH, Heidelberg, Germany, no. 61001	Skalli et al[16]
CR3/43	Human MHC class II molecules (HLA-DP/DQ/DR)	DAKO, Hamburg, Germany, no. M 0775	
	Human sialoadhesin, polyclonal rabbit IgG	Donated by Dr. P. R. Crocker/Dr. A. Hartnell, University of Dundee, UK	Steiniger et al[13] Brinkman-Van der Linden et al[17]
HECA-452	Human CLA, subset of sLe^x carbohydrate determinants in certain selectin-ligands	Pharmingen, Heidelberg, Germany, no. 35821A	Duijvestijn et al[18]
HSN1	Human sialoadhesin, mAb	Donated by Dr. P. R. Crocker/Dr. A. Hartnell, University of Dundee, UK	Steiniger et al[13] Brinkman-Van der Linden et al[17]
	Human IgM, polyclonal rabbit Ig	DAKO, no. A 0425	
	Human IgD, polyclonal rabbit Ig	DAKO, no. A 0093	
	Human CD3 ϵ chain (aa 156–168), polyclonal rabbit Ig	DAKO, no. A 0452	
JC/70A	Human CD31 (PECAM-1), expressed on endothelia and other cells	DAKO, no. M 0823	Parums et al[19]
JCB117	Human CD79a (Ig-alpha or mb-1), signal-transducing molecule associated with membrane Ig	DAKO, no. M 7050	
KiM1-P	Human CD68 (macrosialin), expressed by most monocytes and macrophages	Donated by Dr. M. R. Parwaresch, University of Kiel, Germany	Radzun et al[20]
KiM2	Human monocytes, certain macrophages and granulocytes, antigen unknown	Donated by Dr. M. R. Parwaresch, University of Kiel, Germany	Radzun et al[21]
Ks 18.04	Human cytokeratin 18	Progen GmbH, Heidelberg, Germany, no. 61028	
L26	Human CD20, putative Ca^{++} channel expressed primarily on B-cells	DAKO, no. M 0755	Mason et al[22]
MECA-79	Mouse PNAd, carbohydrate determinant in certain L-selectin ligands, cross-reacts with human	Pharmingen, no. 09961D	Streeter et al[23]
MϕP-9	Human CD14 (Leu-M3), expressed by monocytes, granulocytes (weakly) and macrophage subpopulations, acts as receptor for bacterial lipopolysaccharide	Becton Dickinson, Heidelberg, Germany, no. 7490	
MNF116	Human cytokeratins 5, 6, 8 and 17	DAKO, no. M 0821	
QBEnd10	Human CD34, class II epitope	DAKO, no. M 7165	
SMMS-1	Human smooth muscle myosin	DAKO, no. M 3558	
TK8-14	Human VAP-1	Bender MedSystems, no. BMS 167, via Biozol, Eching, Germany	Salmi and Jalkanen[24]
TM 1009	Human CD141 (thrombomodulin)	DAKO, no. M 0617	

complex for 30 minutes at room temperature. After washing, peroxidase activity was revealed using diaminobenzidine (DAB) and the sections were then dehydrated and coverslipped in Eukitt.

mAb CR3/43 against human MHC class II molecules was visualized by a tyramide-enhanced ABC method on paraffin sections. The mAbs directed against CD79a, CD4, CD8, against cytokeratins and immunoglobulins as well as mAbs MECA-79 and HECA-452 were used on paraffin sections that had been autoclaved on silanized slides for 20 minutes in citrate buffer. mAbs KiM1-P and asm-1 produced a somewhat more extensive staining in autoclaved as compared to enzyme-treated paraffin sections. mAb Ks 18.04 was used on autoclaved paraffin sections that had been treated with trypsin.

If formol pigment was unacceptable, paraffin sections were treated with 1% NH_4OH in 70% ethanol for 5 minutes at room temperature after color development with DAB and nuclear counterstaining.

Double-Staining Procedure for Immunohistology

Co-expression of two antigens cannot be directly demonstrated by immunoenzymatic staining for light microscopy. We thus used subtractive staining methods designed in a way that the chromogen of the first incubation step blocks all subsequent antibody binding and visualization. By reversing the sequence of antibody application (not described in detail below) this method demonstrates whether single positive cells are present or not. Appropriate controls include omission of first or second primary antibody and of both primary antibodies.

Double Staining with mAbs KiM1-P and HSN-1

Double staining using the CD68 antibody KiM1-P and mAb HSN-1 against sialoadhesin was performed on paraffin sections to prove that the sialoadhesin-positive cells were macrophages.

mAb KiM1-P was visualized first using the ABC method and DAB as described above. After appropriate washes, mAb HSN-1 supernatant was diluted 1:10 in PBS/bovine serum albumin/NaN_3 and applied for 1 hour at room temperature. HSN-1 was revealed by rabbit anti-mouse Ig (1:30 in PBS for 30 minutes) and mouse alkaline phosphatase anti-alkaline phosphatase (APAAP)-complexes (1:40 in PBS for 30 minutes). Incubation with anti-Ig and APAAP-complexes was repeated once to enhance staining. Finally, deposition of APAAP complexes was revealed using fast blue BB as described below, but including levamisol in the AS-MX-phosphate buffer.

Double Staining with mAb Asm-1 and anti-CD3 Serum or mAbs Asm-1 and 10A3

For double staining of mAb asm-1 detecting smooth muscle α-actin and a rabbit anti-human CD3 serum (DAKO no. A 0452; DAKO, Glostrup, Denmark) on paraffin sections, asm-1 was first detected by an ABC technique using alkaline phosphatase (Vectastain elite kit, AP, no. AK-5000; Vector Laboratories). Asm-1 was diluted 1:50 in PBS/bovine serum albumin/NaN_3 with avidin and incubated for 60 minutes. Biotinylated rabbit anti-mouse Ig was applied at 1:200 in PBS/biotin/5% human serum for 30 minutes. After washing, complexes of avidin and biotinylated alkaline phosphatase (AB-AP) were used 1:100 in PBS. The presence of alkaline phosphatase complexes was revealed by nitro blue tetrazolium (Sigma no. N-6639) using 5-bromo-4-chloro-3-indolyl phosphate (BCIP) (Sigma no. B-8503). Nitro blue tetrazolium was dissolved in 70% dimethylformamide/bidistilled water, BCIP was dissolved in 100% dimethylformamide and added to Tris-buffer, pH 9.5, with levamisol (100 mmol/L Tris, 50 mmol/L $MgCl_2$, 100 mmol/L NaCl, 1 mmol/L levamisol) to give a final concentration of 0.42 mmol/L nitro blue tetrazolium and 0.40 mmol/L BCIP. The sections were incubated with the chromogen solution for 12 to 14 minutes at room temperature and controlled microscopically. After washing, the rabbit anti-human CD3 serum was added and revealed by the ABC procedure using peroxidase and DAB as chromogen. The slides were finally embedded in Mowiol and photographed immediately. mAbs asm-1 and 10A6, which are directed against MAdCAM-1, were used in a similar procedure on isopropanol-fixed cryosections.

Demonstration of Acid Phosphatase in Cryostat Sections

Acid phosphatase activity was detected in cryostat sections according to the method of Burstone and Barka. Briefly, 400 mg pararosaniline-chloride (no. 41680-0250; Acros Organics, NJ) were dissolved in 10 ml 2 N HCl and filtered. Four hundred mg of $NaNO_2$ were dissolved in 10 ml of bidistilled water. Two hundred fifty μl of pararosaniline solution were added to 250 μl of $NaNO_2$ solution and allowed to react for 1 to 2 minutes. The mixture was then immediately diluted with 20 ml of veronal-acetate buffer, pH 7.6. Ten mg of naphthol-AS-biphosphate (Sigma no. 2125) were dissolved in 1 ml of *N,N*-dimethylformamide and added to the buffered pararosaniline solution. The pH was adjusted to 5.0 and the solution warmed to 37°C. Cryostat sections were fixed for 10 minutes in Baker's formol-calcium at 4°C, washed in bidistilled water and incubated for 15 minutes at 37°C in the prewarmed hexazotized pararosaniline/naphthol-AS-biphosphate solution. The sections were then washed with distilled water, counterstained with Mayer's hemalum and coverslipped in Mowiol.

Demonstration of Alkaline Phosphatase in Cryostat Sections

Cryostat sections were fixed in cold isopropanol for 10 minutes and incubated in the dark for 20 minutes at room temperature with 1 mg/ml fast blue BB salt (Sigma no. F 3378) in naphthol AS-MX-phosphate buffer. The buffer was prepared by dissolving 2 mg of naphthol AS-MX-phosphate (Sigma no. N 4875) in 0.2 ml of dimethylfor-

mamide (Merck no. 3034) and adding this solution to 9.8 ml 0.1 mol/L Tris-HCl buffer, pH 8.2. The fast blue solution was filtered before use. The sections were counterstained with nuclear fast red and mounted in Mowiol.

Results

Species-Specific Structure of the MZ in Humans

The human splenic MZ exhibits great interindividual variability (Figure 1; A, B, and C). In most specimens it is predominantly composed of large CD20- and surface IgM-positive B lymphocytes, which appear pale after hematoxylin and eosin (H&E) staining. The expression of IgD in these cells varies individually, ranging from low to absent (Figure 1; A, B, and C). This phenotype resembles that of memory B lymphocytes described in rodent MZs. The human MZ does, however, also harbor strongly IgD-positive recirculating B cells. These cells form individually variable patterns in the MZ. In some spleens strongly IgD-positive recirculating B cells occur as a prominent ring structure in the outer MZ, which continues along the PALS (Figure 1A). In most specimens there are, however, only a few strongly IgD-positive cells scattered over the entire MZ and cells of this phenotype are almost absent around the PALS (Figure 1B). Interestingly, B cells with a memory phenotype (IgM-positive/IgD-negative or weakly positive) are predominantly found around the follicles and are difficult to recognize around the PALS (Figure 1B). A visible border between the primary follicle, respectively, the strongly IgD-positive mantle zone of a secondary follicle, and the MZ does not occur in humans (Figure 1; A, B, and C). This is partially because of the absence of a marginal sinus and the accompanying marginal metallophilic macrophages, which separate the compartment of migratory B lymphocytes from the MZ in rats.[13] There is no reactivity for CD31 (PECAM-1) or CD34 between mantle zone and MZ or within the MZ (Figure 1D). The adhesion molecule sialoadhesin, which is characteristic of marginal metallophilic macrophages and MZ macrophages in rats is not expressed in the human MZ or mantle zone, although CD68 and/or acid phosphatase-positive macrophages are clearly present in both regions.[13]

In distinction to rats, the MZ is often, but not always, divided into a broad inner and a smaller outer compartment by one or several layers of pale-staining elongated cells that are visible in H&E-stained paraffin sections. These cells also show up as pale unstained structures in follicles incubated with CD20 or CD79a. Both MZ compartments are enhanced by these reagents, because B lymphocytes in the outer MZ stain much more intensely than B cells in the inner part of the MZ (Figure 1E).

The elongated cells subdividing the MZ reveal a rather peculiar phenotype. They are strongly positive for smooth muscle α-actin, for smooth muscle myosin, for alkaline phosphatase, for thrombomodulin (CD141), probably for Thy-1 (CD90), for cytokeratin 18, and as demonstrated by staining with mAb MNF116, for at least an additional cytokeratin, and, probably, also for VCAM-1 (CD106) and VAP-1 (Figure 1, F and G). By subtractive double staining it is evident, that these cells also express MAdCAM-1 (data not shown). The cells exhibiting this phenotype continue into the T cell zone forming a network within the PALS, which is often most strongly reactive in the outer PALS. The staining pattern is individually variable and not identical with all reagents mentioned, because the number of elongated-branched cells detected in the MZ differs. In some specimens only a relatively small rim of cells is strongly positive for smooth muscle α-actin, smooth muscle myosin, and the other antigens in the MZ. Weaker reactivity for actin and myosin as well as strong reactivity for cytokeratin 18, Thy-1, VCAM-1, and MAdCAM-1 may, however, also occur in a much broader region and partially or entirely extend into the perifollicular zone (Figure 1F and Figure 2, F and G). In the MZ the strongly smooth muscle α-actin-positive cells are often intimately associated with a ring-like accumulation of CD4- and CD3-positive T lymphocytes (Figure 2, A and B). In contrast, CD8-positive T lymphocytes are only sparsely distributed in the MZ and do not accumulate in this compartment (Figure 2C).

The Human Perifollicular Zone: An Intermediate Compartment between White and Red Pulp

In conventionally stained paraffin sections an additional compartment surrounding the follicular MZ is visible, which we term the "perifollicular zone" according to van Krieken and te Velde,[2,25] who introduced this name. In paraffin sections the perifollicular zone is often distinguished by accumulations of erythrocytes outside the MZ (Figure 2D). This region also harbors sheathed capillaries in addition to a few scattered nonsheathed CD34- and/or CD31-positive capillaries (data not shown). The outer part of the perifollicular zone intermingles with the red pulp and contains the beginnings or ends of sinuses. The perifollicular zone may thus also be regarded as a specialized part of the red pulp surrounding the follicles. Interestingly, the expression of CD34, which is almost absent in most red pulp sinus endothelia in paraffin and cryosections, is enhanced in the perifollicular sinuses (Figure 1D).

The sheathed capillaries in the perifollicular zone are covered by a one- or two-layered sheath of macrophages. These macrophages co-express the adhesion molecule sialoadhesin and CD68 as demonstrated by double staining with mAb KiM1-P and a polyclonal antiserum or mAb HSN-1 against sialoadhesin.[13,26] The capillary sheaths are also positive for acid phosphatase, but do not express class II MHC molecules. In certain specimens capillary sheaths are absent, but instead strongly sialoadhesin-positive single macrophages occur scattered in the perifollicular zone (Figure 2E).

Besides erythrocytes, CD15-positive granulocytes and CD14-positive monocytes normally accumulate in the perifollicular zone.[26] All these blood cells are observed within spaces that are not lined by endothelia but by fibers and fibroblasts. This phenomenon is also found in

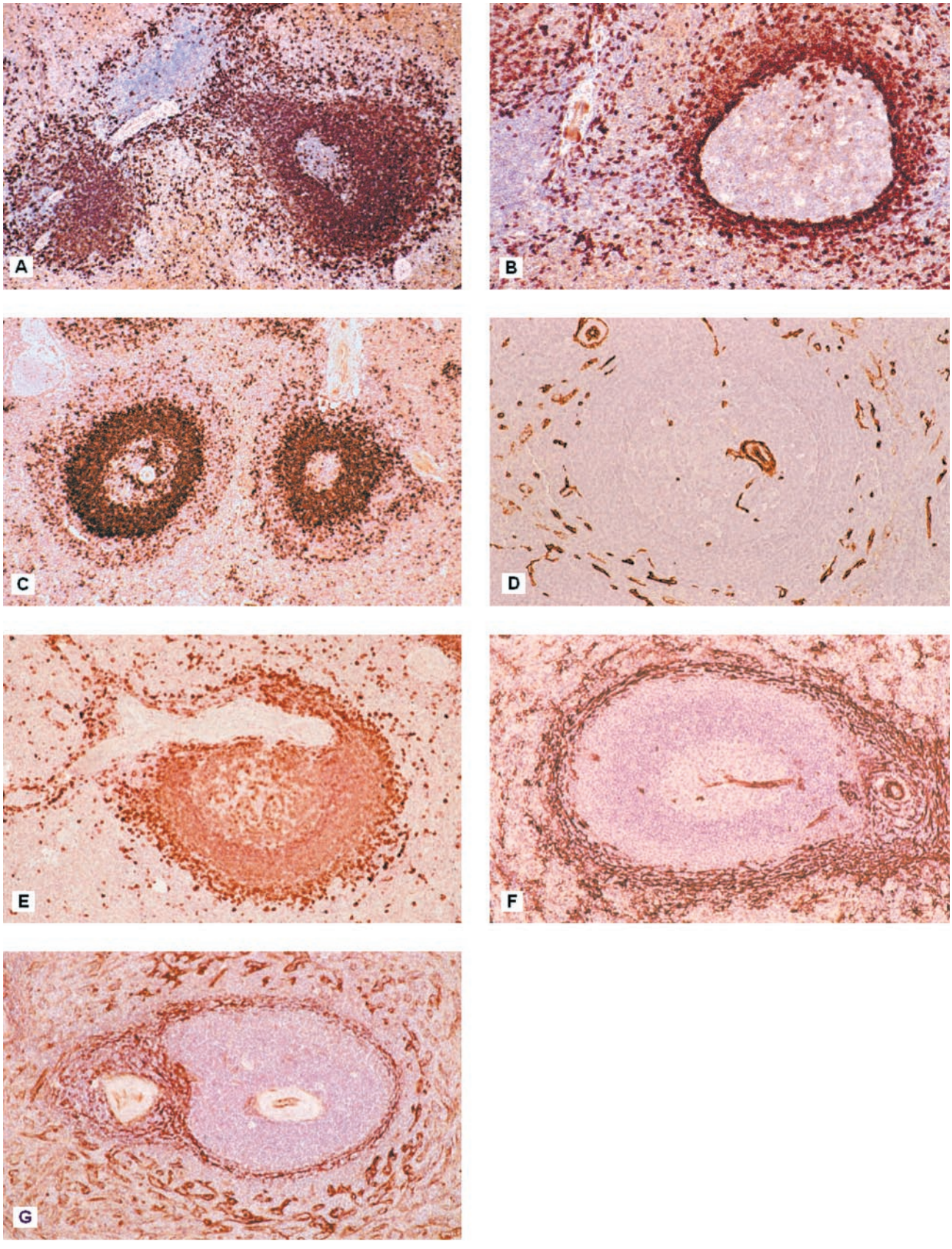
A
B
C
D
E
F
G

autopsy specimens. The fact that blood cells are contained in an open part of the splenic circulation in the perifollicular zone is not only demonstrated by the distribution pattern of CD31, CD34, and CD141, but is supported by additional evidence coming from adhesion molecules involved in lymphocyte recirculation.

Neither mAb MECA-79, directed against sulfated carbohydrate determinants in several glycoproteins summarized as peripheral node addressin nor mAb HECA-452, detecting a sialyl-Le^x epitope in the context of several proteins named cutaneous lymphocyte antigen reveal any vessel-like structures in the perifollicular zone. Likewise, P-selectin and E-selectin are not detectable in this area. Interestingly, a gut-specific ligand for L-selectin and $\alpha 4\beta 7$ integrin, MAdCAM-1, demonstrated by mAbs 10A6 and 10G3, is present in a broad stripe of strongly stained branched cells in the outer MZ and also in the perifollicular zone. As demonstrated in Figure 2, F and G, mAb 10A6 visualizes a fine meshwork of branched positive cells in the perifollicular zone and coarser more strongly stained meshes of cells in the MZ and in the PALS. The extent of the ring-like perifollicular MAdCAM-1 reactivity is individually variable. It is very likely that similar to the double-positive elongated cells in the MZ, most MAdCAM-1-positive cells in the perifollicular zone are also positive for smooth muscle α-actin. This is, however, difficult to assess with certainty, because some cells in the perifollicular zone stain only weakly for smooth muscle α-actin. Higher magnification of cryosections reveals that the MAdCAM-1-positive cells in all regions ensheath unstained bundles of fibers (Figure 2H). The distribution of the MAdCAM-1-positive cells appears at least partially coincident with the strongly stained ring of Thy-1-positive branched cells around the follicles. Double staining for Thy-1 was, however, not possible because of diffusion artifacts most likely caused by dissolution of the lipid membrane anchor of this molecule after isopropanol fixation of cryosections. The cells positive for Thy-1 and/or MAdCAM-1 and the other antigens mentioned do not stain for prolyl-hydroxylase. Thus, they most likely represent inactive fibroblasts.

In addition to erythrocytes, granulocytes, and monocytes, in some specimens with full-blown germinal centers large numbers of CD20- and CD79a-positive B lymphocytes, which are negative or weakly positive for IgD, extend from the MZ into the perifollicular zone.[13] The perifollicular zone is also distinguished from the red pulp by the absence or extremely low number of plasmablasts and plasma cells as shown by absence of staining for intracellular IgM using highly diluted antibodies in autoclaved paraffin sections. Interestingly, accumulations of T lymphocytes positive for CD4 and CD3 are not observed in the perifollicular zone, but only in the MZ.

Discussion

In rats and in man the blood flow through the spleen is unique, because it passes an open and a closed circulation in parallel. The splenic red pulp cords are formed by fibroblasts and reticular fibers. They represent the open part of the splenic circulation that receives blood from terminal arterioles and lacks endothelia. The closed part of the splenic circulation consists of the rest of the vascular tree including the splenic red pulp sinuses. Despite this classification, the sinuses have an unusual discontinuous endothelium and basement membrane,[27] which permit erythrocytes to enter from the open circulation of the surrounding cords.[28]

Our results show, that the border between the splenic white and red pulp is more sophisticated in humans than in rats or mice. They provoke the interpretation that the region where red and white blood cells enter the spleen is species-specific. Recirculating mouse and rat lymphocytes are imagined to enter the white pulp by adherence to the endothelium of the marginal sinus and by migration across the MZ.[29–31] Thus, they have to cross the wall of a vessel belonging to the closed splenic circulation.

We speculate that in humans the entry of white blood cells into the splenic white and red pulp is different in that it occurs primarily via the open splenic circulation in the perifollicular zone. Thus, the white cells need not cross an endothelium, because terminal vessels directly open into this site. Vascular structures similar to the rodent marginal sinus do definitively not exist in humans. We can, however, not exclude that the few capillaries in the perifollicular zone that express CD31 and/or CD34 serve the exit of white blood cells. These vessels are, however, only sparsely distributed.

Figure 1. A–C: Variable distribution of surface IgD-positive B cells in individual specimens (ABC technique on autoclaved paraffin sections using polyclonal anti-human IgD). **A:** Strongly IgD-positive recirculating B cells occupy the mantle zones of two tangentially sectioned secondary follicles. In this case strongly IgD-positive cells are densely distributed in the inner MZ, obscuring the memory B cells that are only weakly positive for surface IgD. Strongly IgD-positive B cells occur in the outer MZ and extend along the PALS (**top left**) as a small stripe. Final magnification, ×55. **B:** Strongly IgD-positive recirculating B cells form a small mantle zone in the secondary follicle. The inner MZ is occupied by weakly IgD-positive memory B cells mixed with few strongly IgD-positive cells. The outer MZ is hardly recognizable. There are only few strongly IgD-positive B cells at the periphery of the PALS (**left**). Final magnification, ×88. **C:** A broad IgD-positive mantle zone surrounds the unstained germinal centers of two secondary follicles. The memory B cells of the inner MZ are IgD-negative in this specimen. A prominent ring-like accumulation of strongly IgD-positive B cells is seen in the outer MZ, whereas fewer of these cells are scattered in the inner MZ. Strongly IgD-positive B cells are almost absent at the periphery of the PALS. Final magnification, ×55. **D:** Distribution of CD34 in a secondary follicle. Few endothelia and perivascular fibroblasts are stained in the follicle interior. CD34 is not detected between the mantle zone and the MZ, indicating absence of a marginal sinus. A few capillary endothelia are reactive in the perifollicular zone. Weakly CD34-positive sinus endothelia occur only in this region. ABC technique on paraffin section using mAb QBend10. Final magnification, ×110. **E:** B lymphocytes stained for CD79a. All compartments of the secondary follicle are positive. The reactivity is most pronounced in the outer MZ. ABC technique on autoclaved paraffin section using mAb JCB117. Final magnification, ×69. **F:** Smooth muscle α-actin in a secondary follicle: A network of strongly actin-positive branched cells divides the inner MZ from the outer MZ. In this specimen a relatively large part of the outer MZ contains actin-positive cells. More weakly stained cells are present in the perifollicular zone. The actin-positive branched cells continue into a network filling the entire PALS (**right**). The red pulp also harbors some actin-positive cells. ABC technique on autoclaved paraffin section using mAb asm-1. Final magnification, ×88. **G:** Thrombomodulin in a primary (or tangentially sectioned secondary) follicle. Thrombomodulin-positive branched cells occur at the border between inner MZ and outer MZ and continue into the PALS (**left**). Red pulp sinus endothelia are also thrombomodulin-positive, especially in the perifollicular region. ABC technique on paraffin section using mAb TM 1009. Final magnification, ×69.

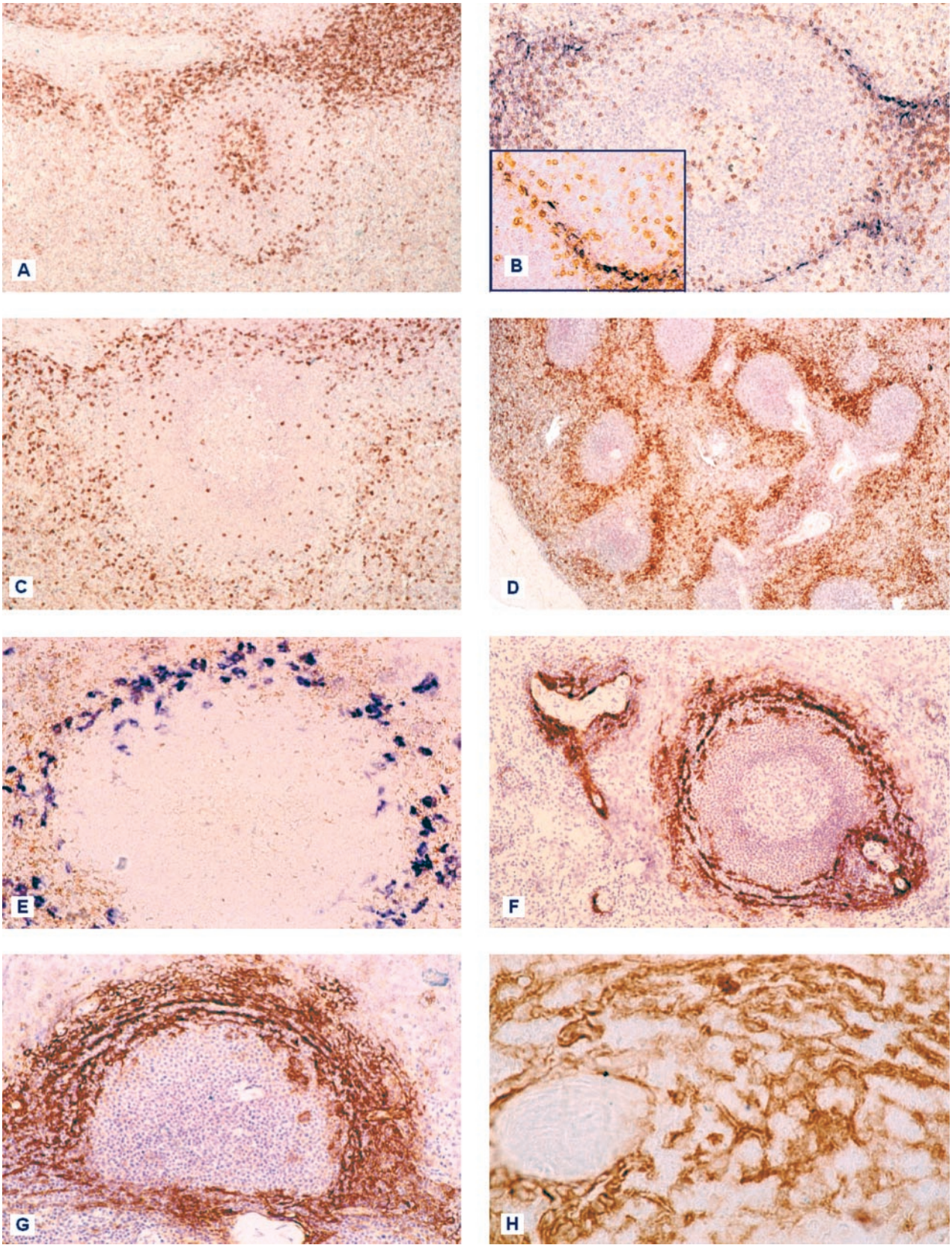
A
B
C
D
E
F
G
H

Irrespective of how the perifollicular zone is reached, this region clearly belongs to the open part of the splenic circulation where blood is located in spaces without an endothelial lining. It is thus not astonishing that the fibroblasts forming the stroma of the perifollicular zone and the MZ acquire qualities of endothelial cells. They do not only express Thy-1, but to a variable extent also thrombomodulin, VCAM-1, VAP-1, or MAdCAM-1. With the exception of some dermal vessels and of lymph node HEVs,[32] Thy-1 has only been demonstrated in human fibroblasts, but not in normal human endothelia.[15] That the cells carrying these antigens cannot be classified as endothelial cells is also supported by their morphology. As demonstrated in Figure 2H, the MAdCAM-1-positive cells ensheath bundles of fibers, but do not form vessel-like spaces. In addition, similar to the VCAM-1- and VAP-1-positive cells, the MAdCAM-1-positive cells continue into the PALS in a reticular pattern. Thus, they also occur in a region where no extensive vascular plexus exists. This distribution pattern corresponds to that of fibroblastic reticulum cells described in the past.[33] The detectability of the different antigens in the fibroblasts is individually variable, e.g., in some specimens only a small population in the MZ is strongly positive for smooth muscle α-actin, myosin, and MAdCAM-1, whereas in others the positive cells extend from the outer MZ through to the perifollicular zone. The significance of the peculiar microfilament and intermediate filament pattern in splenic fibroblasts is open to speculation. Microfilaments may alleviate the contact of fibroblasts to reticular fibers by inhibiting the diffusion of transmembrane adhesion molecules. An intimate contact to reticular fibers may be of special importance at the beginning of the open splenic circulation.

Thus, although HEVs do not occur in human spleens, adhesion molecules typically expressed in HEVs of the mucosa-associated lymphatic system such as MAdCAM-1[34] together with adhesion molecules of a broader distribution such as VCAM-1[35] and VAP-1[24] are present. In contrast, antibodies MECA-79 and HECA-452 do not react with fibroblasts or endothelia in the spleen. MECA-79 is directed against the peripheral node addressin and HECA-452 reacts with the cutaneous lymphocyte antigen. Both reagents recognize carbohydrate determinants occurring in different proteins present in HEVs of mucosal and nonmucosal lymphatic tissue.[18,23,36,37] These determinants also form the ligands for selectins. Missing reactivity with MECA-79 and HECA-452 might indicate that the shear forces in the open circulation of the perifollicular zone are minimal and thus do not necessitate the presence of the whole range of selectin ligands required for lymphocyte adhesion in HEVs. Reactivity with MAdCAM-1 antibodies 10A6 and 10G3 in the human spleen has been noted by Briskin and colleagues.[14] These authors did, however, regard the MAdCAM-1-positive cells as sinus endothelia.

In many, but not in all, specimens CD4-positive T lymphocytes accumulate close to the ring of fibroblasts stained for smooth muscle α-actin, MAdCAM-1, and other antigens in the MZ. This phenomenon has obviously led to the erroneous assumption that the MZ is a T cell region.[38] We should like to interpret this finding as indicating CD4 T cell immigration into the white pulp via the MZ and its fibroblasts (see below). Why CD8-positive T lymphocytes do not accumulate in a ring-like manner in the MZ, can, however, not be explained. In fact, there are only very few CD8-positive cells in the MZ and within follicles. Apart from the PALS, where CD8-positive cells form a minority of T lymphocytes, most of the CD8-positive cells occur in the red pulp, where a certain number may in fact represent natural killer cells. The distribution may thus indicate that immigration of CD8-positive T cells into the white pulp differs quantitatively or qualitatively from that of CD4-positive T lymphocytes.

We can, of course, not be sure that the fibroblasts are the only cell type focusing CD4-positive T cells to the MZ. From own unpublished studies we are aware of the fact that branched cells with a phenotype similar to immature dendritic cells occur in close proximity to the special smooth muscle actin-positive fibroblasts.

The role of the strongly sialoadhesin-positive macrophages in the capillary sheaths and in the perifollicular zone is far from clear. We speculate that these cells represent the human equivalent of the rodent marginal metallophilic and MZ macrophages.

The qualitative findings described in this article are more or less invariant among different individuals. However, there is substantial interindividual variation with re-

Figure 2. A: CD4-positive T lymphocytes in a secondary follicle. **Top:** A longitudinal and partially tangential section of the PALS. Many CD4-positive T cells are present in the germinal center, whereas only few CD4-positive T cells occur in the mantle zone and in the inner MZ. A prominent ring-like accumulation of CD4-positive T cells occurs at the border between inner MZ and outer MZ. ABC technique on autoclaved paraffin section using mAb 1F6. Final magnification, ×69. **B:** Double staining for smooth muscle α-actin (dark blue) and CD3 (brown) in a degenerating secondary follicle. **Inset** shows a 1.4-fold magnification of the **top right** part of the figure. CD3-positive T cells are closely associated with the most strongly smooth muscle α-actin-positive branched cells in the MZ. The PALS is situated on the right and left side of the follicle. mAb asm-1 is highly diluted to permit better visualization of the apposed CD3-positive cells. APAAP technique with nitro blue tetrazolium/BCIP for mAb asm-1 and ABC with DAB for CD3 antiserum. Final magnification, ×110. **C:** CD8-positive cells in the same secondary follicle as shown in **A**. CD8-positive cells do not accumulate in the follicle. Many small round cells and sinus endothelia are stained in the red pulp. ABC technique on autoclaved paraffin section using mAb 4B11. Final magnification, ×69. **D:** Erythrocytes in the perifollicular zone demonstrated by DAB. A similar pattern is revealed by staining for CD14 or CD15. Final magnification, ×28. **E:** Strongly sialoadhesin-positive macrophages (blue) scattered in the perifollicular zone. The brown background staining is because of residual peroxidatic activity of erythrocytes outlining the perifollicular zone. Cryosection without nuclear counterstain. mAb HSN-1 revealed by an APAAP technique with fast blue, erythrocytes are stained by DAB. Final magnification, ×110. **F:** MAdCAM-1-positive cells in a secondary follicle and PALS. Rows of strongly MAdCAM-1-positive branched cells occur at the border of the inner and outer MZ. More weakly staining cells are located in the outer MZ and perifollicular zone. MAdCAM-1-positive cells also form a network in the PALS (**right**). ABC technique on cryosection using mAb 10A6. Final magnification, ×69. **G:** Primary (or tangentially sectioned secondary) follicle stained for MAdCAM-1. In this specimen more branched cells are positive for MAdCAM-1 than in **F**. There are strongly positive elongated cells in the outer MZ and more weakly staining cells with finer and more elaborate projections in the perifollicular zone. The PALS is located at the bottom. ABC technique on cryosection using mAb 10A6. Final magnification, ×110. **H:** Higher magnification of MAdCAM-1-positive cells in the PALS. A central arteriole is located to the **left**. The MAdCAM-1-positive branched cells ensheath bundles of fibers that appear as pale stripes within the brown envelope of immunoreactive cells. No nuclear counterstain. ABC technique on cryosection using mAb 10A6. Final magnification, ×277.

spect to the quantity of cells of a given phenotype. Variability in cellular composition is a special feature of human spleens, which does not occur in inbred rodents, and which has been noted by all authors investigating major numbers of specimens, even with conventional staining techniques. In the 30 spleens removed after traumatic rupture, variation in the numbers of T cells in the MZ, in the IgD-positive B cells at the periphery of the PALS, or in the width of the area of MZ fibroblasts did not correlate with a pre-existing disease. The vast majority of the spleens had a normal weight and the accident was severe, causing a polytrauma. Thus, it is most likely that individually different recirculation kinetics or short-term effects during surgical treatment, such as responses to drugs or stress, are responsible.

Our findings are also valid for autopsy specimens. Thus, it is highly unlikely that the microanatomic compartments we describe, for example the perifollicular zone, are caused by artifacts such as perifollicular hemorrhage.[39] The broad selection of specimens and, in addition, the very peculiar expression of adhesion molecules such as MAdCAM-1 in perifollicular and MZ fibroblasts coincident with an accumulation of leukocytes strongly argue against an erroneous interpretation of the morphological findings.

Overall, our demonstration of a special compartment at the border of white and red pulp in humans is in accordance with the findings of van Krieken and te Velde,[2,25] who introduced the term "perifollicular zone." Although the *in vitro* phenotype of MZ B lymphocytes is well defined in humans,[40,41] there has been much confusion about the microanatomical location of these cells, because the MZ has often been mixed up with the perifollicular zone.[42–44] There may, in fact, be conditions in which the perifollicular zone harbors major numbers of B lymphocytes making a distinction between outer MZ and perifollicular zone rather difficult. Our findings clearly disagree with the interpretations by Hsu and colleagues[38,45] in that we definitively show the human MZ as a B-lymphocyte region with a variable content of CD4-positive T lymphocytes. Apart from these two studies, the majority of other immunohistological reports on the human splenic white pulp correspond to our results.[1–4,46,47] With exception of the study by van Krieken and te Velde,[2] the existence of the perifollicular zone went, however, undetected in all these investigations. This is also true for the publications of Buckley and colleagues,[5,6] who investigated the distribution of macrophages and dendritic cells in human spleens and described accumulations of monocytes or granulocytes around the follicles.

The apparent absence of a marginal sinus in humans contradicts the reports of Schmidt and colleagues[48,49] and Yamamoto and colleagues[50] using vascular corrosion casts. We assume that the marginal sinus demonstrated by these authors represents in fact the spaces of the perifollicular zone filled by casting material. This is rather likely, because during the casting procedure all lymphocytes are digested away, so that proper orientation in the specimen is impossible.

A special stromal cell type has been noted in the human splenic MZ by several investigators, who described expression of smooth muscle α-actin, cytokeratin 8 and/or 18, and smooth muscle myosin and Thy-1.[32,51–54] Interestingly, Timens and Poppema[1] also found CD4-positive cells located in a ring-like manner in the human MZ. These authors and Grogan and colleagues[3] detected differences in the distribution of CD4-positive and CD8-positive T cells in the spleen.

Our findings are best explained by the following hypothesis: in humans the outermost compartment of the follicles, the perifollicular zone, is part of the open splenic circulation and represents the entry compartment for recirculating lymphocytes into the white pulp. Entry of CD4-positive T lymphocytes does not require adhesion to endothelial cells, but depends on special stromal fibroblasts with an endothelial-like phenotype secreting lymphocyte-attracting chemokines and guiding the T cells into the PALS. The phenotypic features of these fibroblasts are concomitantly regulated by the CD4-positive T lymphocytes passing along. The number of fibroblasts with a given phenotype may thus vary according to the activation state of the recirculating T cells. Another type of fibroblasts may interact with recirculating strongly IgD-positive B lymphocytes, arresting them in the outer MZ and along the PALS. Similar to CD4-positive T cells, the number and location of recirculating IgD-positive B cells in the MZ depends on the individual dynamics of lymphocyte immigration. Erythrocytes, granulocytes, and monocytes do not respond to the chemokines secreted by the fibroblasts. After initial adhesion, these cells leave the perifollicular zone in the opposite direction and enter the red pulp cords.

Acknowledgments

We thank Dr. M. Briskin, Leukosite Inc., Cambridge, MA, for generous gifts of mAbs 10A6 and 10G3; Dr. P. R. Crocker and Dr. A. Hartnell, Institute of Biochemistry, University of Dundee, UK, for donating polyclonal and monoclonal anti-human sialoadhesin antibodies; Dr. M. R. Parwaresch and Dr. H.-H. Wacker, Institute of Pathology, University of Kiel, Germany, for providing mAbs KiM1P and KiM2; Dr. V. Grau, Institute of Anatomy and Cell Biology, University of Marburg, Germany, for helpful discussions on details of staining techniques; B. Herbst for providing excellent technical assistance; and F. Unterstab, Department of Pathology, University of Marburg, for essential contributions to the electronic processing of the figures.

References

1. Timens W, Poppema S: Lymphocyte compartments in human spleen. An immunohistologic study in normal spleens and noninvolved spleens in Hodgkin's disease. Am J Pathol 1985, 120:443–454
2. Van Krieken JHJM, te Velde J: Immunohistology of the human spleen: an inventory of the localization of lymphocyte subpopulations. Histopathology 1986, 10:285–294
3. Grogan TM, Jolley CS, Rangel CS: Immunoarchitecture of the human spleen. Lymphology 1983, 16:72–82
4. Grogan TM, Rangel CS, Richter LC, Wirt DP, Villar HV: Further delin-

eation of the immuno-architecture of the human spleen. Lymphology 1984, 17:61–68
5. Buckley PJ, Smith MR, Braverman MF, Dickson SA: Human spleen contains phenotypic subsets of macrophages and dendritic cells that occupy discrete microanatomic locations. Am J Pathol 1987, 128: 505–520
6. Buckley PJ: Phenotypic subpopulations of macrophages and dendritic cells in human spleen. Scanning Microsc 1991, 5:147–158
7. Veerman AJP, van Ewijk W: White pulp compartments in the spleen of rats and mice. A light and electron microscopic study of lymphoid and non-lymphoid cell types in T- and B-areas. Cell Tissue Res 1975, 156:417–441
8. Dijkstra CD, Döpp EA, Joling P, Kraal G: The heterogeneity of mononuclear phagocytes in lymphoid organs: distinct macrophage subpopulations in the rat recognized by monoclonal antibodies. Immunology 1985, 54:589–599
9. Van Rooijen N, Claassen E, Kraal G, Dijkstra CD: Cytological basis of immune functions of the spleen. Immunocytochemical characterization of lymphoid and non-lymphoid cells involved in the 'in situ' immune response. Prog Histochem Cytochem 1989, 19:1–69
10. Kraal G: Cells in the marginal zone of the spleen. Int Rev Cytol 1992, 132:31–74
11. Gray D, MacLennan ICM, Bazin H, Khan M: Migrant $\mu^+\delta^+$ and static $\mu^+\delta^-$ B lymphocyte subsets. Eur J Immunol 1982, 12:564–569
12. Van den Berg TK, Brevé JJP, Damoiseaux JGMC, Döpp E, Kelm S, Crocker PR, Dijkstra CD, Kraal G: Sialoadhesin on macrophages: its identification as a lymphocyte adhesion molecule. J Exp Med 1992, 176:647–655
13. Steiniger B, Barth P, Herbst B, Hartnell A, Crocker PR: The species-specific structure of microanatomical compartments in the human spleen: strongly sialoadhesin-positive macrophages occur in the perifollicular zone, but not in the marginal zone. Immunology 1997, 92:307–316
14. Briskin M, Winsor-Hines D, Shyjan A, Cochran N, Bloom S, Wilson J, McEvoy LM, Butcher EC, Kassam N, Mackay CR, Newman W, Ringler DJ: Human mucosal addressin cell adhesion molecule-1 is preferentially expressed in intestinal tract and associated lymphoid tissue. Am J Pathol 1997, 151:97–110
15. Saalbach A, Wetzig T, Haustein UF, Anderegg U: Detection of human soluble Thy-1 in serum by ELISA. Fibroblasts and activated endothelial cells are a possible source of soluble Thy-1 in serum. Cell Tissue Res 1999, 298:307–315
16. Skalli O, Ropraz P, Trzeciak A, Benzonana G, Gillessen D, Gabbiani G: A monoclonal antibody against alpha-smooth muscle actin: a new probe for smooth muscle differentiation. J Cell Biol 1986, 103:2787–2796
17. Brinkman-Van der Linden ECM, Sjoberg ER, Juneja LR, Crocker PR, Varki N, Varki A: Loss of N-glycolylneuraminic acid in human evolution. Implications for sialic acid recognition by siglecs. J Biol Chem 2000, 275:8633–8640
18. Duijvestijn A, Horst E, Pals ST, Rouse BN, Steere AC, Picker LJ, Meijer CJLM, Butcher EC: High endothelial differentiation in human lymphoid and inflammatory tissues defined by monoclonal antibody HECA-452. Am J Pathol 1988, 130:147–155
19. Parums DV, Cordell JL, Micklem K, Heryet AR, Gatter KC, Mason DY: JC70: a new monoclonal antibody that detects vascular endothelium associated antigen on routinely processed tissue sections. J Clin Pathol 1990, 43:752–757
20. Radzun HJ, Hansmann M-L, Heidebrecht HJ, Bödewadt-Radzun S, Wacker HH, Kreipe H, Lumbeck H, Hernandez C, Kuhn C, Parwaresch MR: Detection of a monocyte/macrophage differentiation antigen in routinely processed paraffin-embedded tissues by monoclonal antibody Ki-M1P. Lab Invest 1991, 65:306–315
21. Radzun HJ, Parwaresch MR: Differential immunohistochemical resolution of the human mononuclear phagocyte system. Cell Immunol 1983, 82:174–183
22. Mason DY, Comans-Bitter WM, Cordell JL, Verhoeven M-AJ, van Dongen JJM: Antibody L26 recognizes an intracellular epitope on the B-cell associated CD20 antigen. Am J Pathol 1990, 136:1215–1222
23. Streeter PR, Berg EL, Rouse BTN, Bargatze RF, Butcher EC: A tissue-specific endothelial cell molecule involved in lymphocyte homing. Nature 1988, 331:41–46
24. Salmi M, Jalkanen S: Human vascular adhesion protein-1 (VAP-1) is a unique sialoglycoprotein that mediates carbohydrate-dependent binding of lymphocytes to endothelial cells. J Exp Med 1996, 183: 569–579
25. Van Krieken JHJM, te Velde J: Normal histology of the human spleen. Am J Surg Pathol 1988, 12:777–785
26. Steiniger B, Barth P: Microanatomy and function of the spleen. Adv Anat Embryol Cell Biol 1999, 151:1–101
27. Drenckhahn D, Wagner J: Stress fibres in the splenic sinus endothelium in situ: molecular structure, relationship to the extracellular matrix, and contractility. J Cell Biol 1986, 102:1738–1747
28. MacDonald IC, Ragan DM, Schmidt EE, Groom AC: Kinetics of red blood cell passage through interendothelial slits into venous sinuses in rat spleen, analyzed by in vivo microscopy. Microvasc Res 1987, 33:118–134
29. Van Ewijk W, Nieuwenhuis P: Compartments, domains and migration pathways of lymphoid cells in the splenic pulp. Experientia 1985, 4:199–208
30. Nieuwenhuis P, Ford WL: Comparative migration of B- and T-lymphocytes in the rat spleen and lymph nodes. Cell Immunol 1976, 23:254–267
31. Brelinska R, Pilgrim C: Macrophages and interdigitating cells: their relationship to migrating lymphocytes in the white pulp of rat spleen. Cell Tissue Res 1983, 233:671–688
32. McKenzie JL, Fabre JW: Human thy-1: unusual localization and possible functional significance in lymphoid tissues. J Immunol 1981, 126:843–850
33. Müller-Hermelink HK, v. Gaudecker B, Drenckhahn D, Jaworsky K, Feldmann C: Fibroblastic and dendritic reticulum cells of lymphoid tissue. J Cancer Res Clin Oncol 1981, 101:149–164
34. Berg EL, McEvoy LM, Berlin C, Bargatze RF, Butcher EC: L-selectin-mediated lymphocyte rolling on MAdCAM-1. Nature 1993, 366:695–698
35. Berlin-Rufenach C, Otto F, Mathies M, Westermann J, Owen MJ, Hamann A, Hogg N: Lymphocyte migration in lymphocyte function-associated antigen (LFA)-1-deficient mice. J Exp Med 1999, 189: 1467–1478
36. Michie SA, Streeter PR, Bolt PA, Butcher EC, Picker LJ: The human peripheral lymph node vascular addressin. An inducible endothelial antigen involved in lymphocyte homing. Am J Pathol 1993, 143:1688–1698
37. Tu L, Delahunty MD, Ding H, Luscinskas FW, Tedder TF: The cutaneous lymphocyte antigen is an essential component of the L-selectin ligand induced on human vascular endothelial cells. J Exp Med 1999, 189:241–252
38. Hsu S-M, Cossman J, Jaffe ES: Lymphocyte subsets in normal human lymphoid tissues. Am J Clin Pathol 1983, 80:21–30
39. Farhi DC, Ashfaq R: Splenic pathology after traumatic injury. Am J Clin Pathol 1996, 105:474–478
40. Dunn-Walters DK, Isaacson PG, Spencer J: Analysis of mutations in immunoglobulin heavy chain variable region genes of microdissected marginal zone (MGZ) B cells suggests that the MGZ of human spleen is a reservoir of memory B cells. J Exp Med 1995, 182:559–566
41. Tierens A, Delabie J, Michiels L, Vandenberghe P, De Wolf-Peeters C: Marginal-zone B cells in the human lymph node and spleen show somatic hypermutations and display clonal expansion. Blood 1999, 93:226–234
42. Saitoh K, Kamiyama R, Hatakeyama S: A scanning electron microscopic study of the boundary zone of the human spleen. Cell Tissue Res 1982, 222:655–665
43. Brozman M: Outer mantle zone of the follicle in the human spleen. Virchows Arch A Pathol Anat Histopathol 1985, 407:107–117
44. Brozman M: Anatomical pathways from the white to the red pulp in the human spleen. Acta Anat 1985, 121:189–193
45. Hsu S-M: Phenotypic expression of B lymphocytes. III. Marginal zone B cells in the spleen are characterized by the expression of Tac and alkaline phosphatase. J Immunol 1985, 135:123–130
46. Timens W, Boes A, Poppema S: Human marginal zone B cells are not an activated B cell subset: strong expression of CD21 as a putative mediator for rapid B cell activation. Eur J Immunol 1989, 19:2163–2166
47. Tanaka H, Takasaki S, Sakata A, Muroya T, Suzuki T, Ishikawa E: Lymphocyte subsets in the white pulp of human spleen in normal and diseased cases. Acta Pathol Jpn 1984, 34:251–270
48. Schmidt EE, MacDonald IC, Groom AC: Microcirculatory pathways in normal human spleen, demonstrated by scanning electron microscopy of corrosion casts. Am J Anat 1988, 181:253–266

49. Schmidt EE, MacDonald IC, Groom AC: Comparative aspects of splenic microcirculatory pathways in mammals: the region bordering the white pulp. Scanning Microsc 1993, 7:613–628
50. Yamamoto K, Arimasa N, Yamamoto T, Tokuyama K, Kobayashi T, Itoshima T: Scanning electron microscopy of the perimarginal cavernous sinus plexus of the human spleen. Scanning Electron Microsc 1979, 3:763–768
51. Franke WW, Moll R: Cytoskeletal components of lymphoid organs. I. Synthesis of cytokeratins 8 and 18 and desmin in subpopulations of extrafollicular reticulum cells of human lymph nodes, tonsils, and spleen. Differentiation 1987, 36:145–163
52. Toccanier-Pelte M-F, Skalli O, Kapanci Y, Gabbiani G: Characterization of stromal cells with myoid features in lymph nodes and spleen in normal and pathologic conditions. Am J Pathol 1987, 129:109–118
53. Doglioni C, Dell'Orto P, Zanetti G, Iuzzolino P, Coggi G, Viale G: Cytokeratin-immunoreactive cells of human lymph nodes and spleen in normal and pathological conditions. An immunocytochemical study. Virchows Arch A Pathol Anat Histopathol 1990, 416:479–490
54. Satoh T, Takeda R, Oikawa H, Satodate R: Immunohistochemical and structural characteristics of the reticular framework of the white pulp and marginal zone in the human spleen. Anat Rec 1997, 249:486–494